2024 IEEE Power & Energy Society Innovative Smart Grid Technologies Conference (ISGT) | 979-8-3503-1360-4/24/$31.00 ©2024 IEEE | DOI: 10.1109/ISGT59692.2024.10454180

Data-Driven Modeling and Prediction of Transient Dynamics of Microgrids through Dynamic Mode Decomposition with Control

Xinyuan Jiang[1], Yan Li[2], and Daning Huang[3]
[1,2]Department of Electrical Engineering, The Pennsylvania State University, University Park, PA, 16802 U.S.
[3]Department of Aerospace Engineering, The Pennsylvania State University, University Park, PA, 16802 U.S.
Emails: [1]xuj49@psu.edu, [2]yql5925@psu.edu, [3]daning@psu.edu

***Abstract*—Dynamic Mode Decomposition with Control (DMDc) is presented to develop a data-driven modeling approach for microgrids when the accurate mathematical model is unavailable. As a system identification method, it can precisely model and predict the transient response of microgrids subject to large disturbances. A modified DMDc method is introduced to handle the piecewise constant inputs issue. Precautions on applying the method on measurement data are also discussed. Numerical examples on a typical islanded microgrid have demonstrated that local dynamics can be accurately captured through the DMDc-based data-driven model. By requesting a small amount of data, the data-driven modeling is powerful for performing system forecast and data-driven control.**

***Index Terms*—Microgrids, Distributed Energy Resources (DERs), transient dynamics, Dynamic Mode Decomposition with Control (DMDc), data-driven, nonlinear.**

I. Introduction

The development of Distributed Energy Resources (DERs), such as photovoltaic (PV) and wind power, provides a great opportunity to achieve the target of modernizing power systems. As a flexible energy architecture, microgrids have been developed to deploy DERs for seeking an edge toward energy sustainability. Most DERs are integrated into microgrids through power-electronic interfaces such as inverters. Although those distributed interfaces can enable rapid controls of DERs and flexible operations of microgrids [1], they significantly reduce the system's inertia, making microgrids sensitive to disturbances [2]. Consequently, the system's transient stability that is caused by large disturbances is severely undermined. Although transient dynamics has been studied from many aspects and several control approaches have been developed for stabilizing the system's transients, it is still elusive *how to study and predict the system's transient dynamics when an accurate mathematical model of microgrids is unavailable.*

There exist two major categories of approaches to develop a suitable model by using data for monitoring and controlling a dynamical system, namely parameter estimation [3] and black-box system identification [4]. For the parameter estimation, an accurate model of the studied system is assumed to be available, while the parameters of the model need to be estimated from measurement data [3], [5]. Parameters can be well estimated for linear systems. For nonlinear systems like microgrids, high computational resources and a large volume of measurement data are often required for getting a high-fidelity result via optimization. The black-box identification methods identify both model and parameters of the system, like Prony's method [4], Empirical Mode Decomposition [6], and subspace-based state space identification [7]. These identification methods are usually based on an equilibrium point where the small-signal response of the system is used for identifying the system's model. It needs to properly design experiments for efficiently generating informative data.

Among the black-box system identification, Dynamic Mode Decomposition (DMD) is a powerful family. The conventional DMD algorithms identify a linear autonomous system from trajectories of states [8], while preserving the spectral properties of the original system, i.e. the eigenvalues and eigenvectors. The DMD algorithms have also been extended to identify nonlinear autonomous systems using functions of states. The Extended DMD (EDMD) has been shown to be closely related to the Koopman operator theory that generates a global linearization of a nonlinear dynamical system.

The DMD with control (DMDc) has been developed for the identification of linear state-space system [9]. The DMDc is similar to the classical Eigensystem Realization Algorithm (ERA) but is formulated towards the identification of high-dimensional systems, i.e., when the number of observables is equal to or more than the number of states. This is the case for microgrid systems. The EDMD has also been extended to include control, leading to Koopman bilinear systems [10]. However, such algorithms require a large amount of training data and the resulting model may not be amenable for control purposes. In this paper, we modify and apply the DMDc algorithm to the modeling and prediction of transient dynamics of microgrids. The contributions are stated below.

- A data-driven model is developed based on the DMDc method to predict the transient dynamics of microgrids.
- The uniqueness of DMDc are derived with the piecewise constant inputs given as an example.
- Singular Value Decomposition (SVD) truncation is presented to determine the model order and add regularization, simultaneously.

The remainder of this paper is organized as follows: Section II introduces a modified DMDc method, where issues with step function input are discussed. In Section III, tests on a microgrid have demonstrated that the local modes of the test system can be accurately identified by DMDc. Conclusions are drawn in Section IV.

II. Dynamic Mode Decomposition with Control

A. The DMDc Algorithm

The basic assumption of DMDc is that the system state is generated from an linear dynamical system written as

$$\mathbf{x}_{k+1} = \mathbf{A}\mathbf{x}_k + \mathbf{B}\mathbf{u}_k, \tag{1}$$

where $\mathbf{x}_k \in \mathbb{R}^n$ and $\mathbf{u}_k \in \mathbb{R}^q$ are the state and input at the discrete time k respectively. (1) can be obtained from a DAE model of a microgrid system where $\mathbf{x}_k$ in (1) include the original differential and algebraic variables and $\mathbf{u}_k$ is the constant power load inputs. The derivation is given in the appendix.

The training data consists of triplets $(\mathbf{x}(t), \mathbf{x}(t+T), \mathbf{u}(t))$, where the time step T should be small enough to be able to capture the fastest mode of the system. In order to capture the dynamics of nonlinear systems near an equilibrium point with the model in (1), it is thus important to center the linear model at an equilibrium point by subtracting the equilibrium point from the training data. For a single trajectory of the system, its measurement data can be denoted in discrete time as $\left\{(\mathbf{x}_k, \mathbf{u}_k)\right\}_{k=0}^{m}$. Then, we can construct the data matrices as follows

$$\mathbf{X}_1 = \begin{bmatrix}\Delta\mathbf{x}_0 & \Delta\mathbf{x}_1 & \dots & \Delta\mathbf{x}_{m-1}\end{bmatrix}, \tag{2}$$
$$\mathbf{X}_2 = \begin{bmatrix}\Delta\mathbf{x}_1 & \Delta\mathbf{x}_2 & \dots & \Delta\mathbf{x}_{m}\end{bmatrix}, \tag{3}$$
$$\mathbf{\Upsilon} = \begin{bmatrix}\Delta\mathbf{u}_0 & \Delta\mathbf{u}_1 & \dots & \Delta\mathbf{u}_{m-1}\end{bmatrix}, \tag{4}$$

where $\Delta\mathbf{x}_k = \mathbf{x}_k - \bar{\mathbf{x}}$ and $\Delta\mathbf{u}_k = \mathbf{u}_k - \bar{\mathbf{u}}$ are centered at an equilibrium point $(\bar{\mathbf{x}}, \bar{\mathbf{u}})$.

Based on the above data matrices of measurements and the linear system model given in (1), a regression model as follows, where $\hat{\mathbf{G}}$ is the matrix to be determined.

$$\mathbf{X}_2 = \begin{bmatrix}\hat{\mathbf{A}} & \hat{\mathbf{B}}\end{bmatrix}\begin{bmatrix}\mathbf{X}_1 \\ \mathbf{\Upsilon}\end{bmatrix} = \hat{\mathbf{G}}\mathbf{\Omega}. \tag{5}$$

The least squares fit is defined as $\hat{\mathbf{G}} = \mathbf{X_2}\mathbf{\Omega}^{+}$, where superscript $+$ denotes Moore-Penrose pseudo-inverse. It is the optimal solution to the following problems in the case where (5) is consistent (having at least one solution) or where (5) is inconsistent (having no solution):

$$\begin{cases} \min\limits_{\mathbf{G}} \left\|\mathbf{G}\right\|_{\mathrm{F}}^2 \ \text{ s.t. } \mathbf{X}_2 = \mathbf{G}\mathbf{\Omega} & \text{if (5) is consistent} \\ \min\limits_{\mathbf{G}} \left\|\mathbf{X}_2 - \mathbf{G}\mathbf{\Omega}\right\|_{\mathrm{F}}^2 & \text{if (5) is inconsistent} \end{cases} \tag{6}$$

In practice, since the data is from a nonlinear system centered at close but different equilibrium points the regression model (5) is not satisfied by the discrete-time linearization $\mathbf{A}$ and $\mathbf{B}$ of the DAE system in (1), and even if (5) has no solution the underlying model may still be underdetermined. On the other hand, the local dynamics may have a lower rank than the number of state variables used to describe the global nonlinear dynamics. It is thus necessary in many situations to reduce the rank of the data matrix when calculating the pseudo-inverse of $\mathbf{\Omega}$ through singular value decomposition (SVD).

Denote the SVD of $\mathbf{\Omega} = \mathbf{U}\mathbf{\Sigma}\mathbf{V}^*$, where $\mathbf{\Sigma}$ is a diagonal matrix which has a dimension equal to the rank of $\mathbf{\Omega}$. The reduced $\mathbf{\Omega}$ is obtained by truncating the smaller singular values of $\mathbf{\Sigma}$ and at the same time eliminating the corresponding columns in $\mathbf{U}$ and $\mathbf{V}$ to get $\widetilde{\mathbf{\Omega}} = \widetilde{\mathbf{U}}\widetilde{\mathbf{\Sigma}}\widetilde{\mathbf{V}}^*$. And the regularized least squares fit is given by

$$\hat{\mathbf{G}} = \mathbf{X}_2\widetilde{\mathbf{\Omega}}^{+} = \mathbf{X}_2\widetilde{\mathbf{V}}\widetilde{\mathbf{\Sigma}}^{-1}\widetilde{\mathbf{U}}^*, \tag{7}$$

which approximates the solution to the regularized problem [11]

$$\min_{\mathbf{G}} \left\|\mathbf{X}_2 - \mathbf{G}\mathbf{\Omega}\right\|_{\mathrm{F}}^2 + r\left\|\mathbf{G}\right\|_{\mathrm{F}}^2 \tag{8}$$

where r is the threshold for singular value truncation.

Finally, the estimated system matrices $\hat{\mathbf{A}}$ and $\hat{\mathbf{B}}$ are obtained from $\hat{\mathbf{G}}$

$$\hat{\mathbf{A}} = \mathbf{X}_2\widetilde{\mathbf{V}}\widetilde{\mathbf{\Sigma}}^{-1}\widetilde{\mathbf{U}}_1^*, \tag{9}$$
$$\hat{\mathbf{B}} = \mathbf{X}_2\widetilde{\mathbf{V}}\widetilde{\mathbf{\Sigma}}^{-1}\widetilde{\mathbf{U}}_2^*., \tag{10}$$

where the rows of $\mathbf{U} = \begin{bmatrix}\mathbf{U}_1^\mathsf{T} \ \mathbf{U}_2^\mathsf{T}\end{bmatrix}^\mathsf{T}$ is split according to (5).

Several issues that relates to the DMDc method with step function inputs is discussed next.

B. Uniqueness of DMDc with Piecewise Constant Inputs

The input $\mathbf{u}_k$ in the DMDc model (1) include the load disturbances to the system. Assuming that this input is piecewise constant, the condition for the ability to uniquely identify $\mathbf{A}$ can be found by modifying Theorem 4.8 in [12] for the case of affine systems, which has the form $\mathbf{x}_{k+1} = x_k + \mathbf{b}$.

To establish the connection between the DMDc system (1) and the affine system, first assume that the matrix $\mathbf{A}$ has no eigenvalues of 1 so that $\mathbf{I} - \mathbf{A}$ is invertible. Then, the dynamics of (1) can be rewritten as

$$\mathbf{x}_{k+1} - \mathbf{c}_k = \mathbf{A}(\mathbf{x}_k - \mathbf{c}_k) \tag{11}$$

where $\mathbf{c}_k = (\mathbf{I} - \mathbf{A})^{-1}\mathbf{B}\mathbf{u}_k$. Within each piecewise constant period of the input $\mathbf{u}_k$, the DMDc dynamics is linear with a constant bias $\mathbf{c}$. Thus, the DMDc system with piecewise constant input is an affine system whose bias is controlled by the input $\mathbf{u}$. Note that the bias $\mathbf{c}_k$ is the equilibrium point of the model if $\mathbf{A}$ is stable. The linear dependence of the equilibrium $\mathbf{c}$ on the input $\mathbf{u}$ is a local approximation of how the equilibrium of the power system shifts due to load changes, e.g., the P-V plot [13]. The growing equilibrium error farther from the training range can be addressed by introducing successive DMDc or by using a bilinear model [10].

Based on the uniqueness of affine DMD in [12], the uniqueness of the DMDc with piecewise constant inputs is given as follows.

Definition 1 (DMDc Well-Posedness): Suppose the given time series data $\left\{(\mathbf{x}_k, \mathbf{u}_k)\right\}_{k=0}^{N}$ satisfies the linear dynamics $\mathbf{x}_{k+1} = \mathbf{A}\mathbf{x}_k + \mathbf{B}\mathbf{u}_k$, where $\mathbf{x}_k \in \mathbb{R}^n$, $\mathbf{u}_k \in \mathbb{R}^q$, where

979-8-3503-1360-4/24/$31.00 ©2024 IEEE

$\mathbf{A}$ is assumed to be diagonalizable with $r \leq n$ distinct nonzero eigenvalues $\lambda_1, \ldots, \lambda_r$ and eigenvectors $\mathbf{v}_1, \ldots, \mathbf{v}_r$. For piecewise constant input $\mathbf{u}$ which takes values $\boldsymbol{\mu}_0, \ldots, \boldsymbol{\mu}_h$ at times steps $0, N_1, \ldots, N_h \leq N$. We say that the DMDc problem is well-posed if the conditions

1. $\mathbf{A}$ does not have an eigenvalue equal to 1,
2. $\mathbf{x}_{N_i} - \mathbf{c}_{i+1}$ is not orthogonal to $\mathbf{v}_1, \ldots, \mathbf{v}_r$, where $\mathbf{c}_i = (\mathbf{I} - \mathbf{A})^{-1}\mathbf{B}\boldsymbol{\mu}_i$
3. $N_i - N_{i-1} \geq r + 2$, $i = 1, \ldots, h$,
4. The matrix of distinct input vectors $\begin{bmatrix}\boldsymbol{\mu}_0 \cdots \boldsymbol{\mu}_h\end{bmatrix}$ have maximum column rank q,

Theorem 1: (Uniqueness of DMDc) Suppose that the time series data follow linear dynamics (1) with rank r matrix $\mathbf{A}$ and full rank matrix $\mathbf{B}$. Let $\mathbf{A}'$ and $\mathbf{B}'$ be any other matrices with $\mathbf{A}'$ of rank r that satisfies the same dynamics $\mathbf{x}_{k+1} = \mathbf{A}'\mathbf{x}_k + \mathbf{B}'\mathbf{u}_k$ for $k = 0, \ldots, N-1$. If the DMDc problem is well-posed by Definition 1, then $\mathbf{c}'_i = \mathbf{c}_i,\ i = 0, \ldots, h$, $\mathbf{B}' = \mathbf{B}$, and $\mathbf{A}'$ has the same r nonzero eigenvalues and corresponding eigenvectors as $\mathbf{A}$, up to scaling.

A proof sketch is given in the Appendix. Note that the well-posed condition in Definition 1 does not cover dynamics with eigenvalue 1. This is because the mode with eigenvalue 1 is indistinguishable from the bias $\mathbf{c}_k$. For $\mathbf{A}'$ with a rank higher than r, additional eigenvalues of 1's may be incorrectly identified, which causes incorrect bias $\mathbf{c}_k$ and the matrix $\mathbf{B}'$.

A side effect of reducing the singular values in DMDc is that the rank of $\hat{\mathbf{A}}$ can be reduced to be closer to the number of modes of the underlying linear system. If $\hat{\mathbf{A}}$ has a rank that is too high, from the above discussions, the eigenvalues of $\hat{\mathbf{A}}$ can include addition 1's, and the resulting equilibrium point is dependent both on the initial condition as well as the input, rather than depending only on the input as in $\mathbf{c} = (\mathbf{I} - \mathbf{A})^{-1}\mathbf{B}\mathbf{u}$. Moreover, in practice since the DMDc model $\hat{\mathbf{A}}$ is calculated from data, the additional eigenvalues of $\hat{\mathbf{A}}$ cannot be exactly equal to 1, which means that the resulting system will not maintain its equilibrium points on a time scale much larger than N_i, due to the existence of those almost 1 eigenvalues.

III. Numerical Example

A typical microgrid system shown in Fig. 1 is used to test and validate the feasibility of the DMDc method in obtaining a data-driven model for modeling and predicting the operation of microgrids. The test system operates in the islanded mode, i.e., Circuit Breaker is open; thus, the system is sensitive to disturbances due to the integration of power-electronic interfaces. Because Micro-Turbine has a large power capability, in the test, bus 6 is set as the swing bus. Double-loop controllers are used to control the DERs [14]. All the five power loads are constant power type.

The training data is simulated from the DAE model of the test microgrid with time step $\Delta t = 1$ ms and include two initial condition responses where load changes are introduced from a nominal equilibrium operating point. The two inputs are chosen as the active power changes of Load 5 and Load 6, and two input changes chosen for training data are shown as arrows in the input space shown in Fig. 8. The state variables for the DMDc model (1) are selected as the state variables of the DER controllers (excluding the PLL states) and the real and imaginary parts of every bus voltage phasor xy coordinates.

A. Removal of Angle Shift Invariance

The eigenvalues of the linearization of the microgrid DAE model are plotted as blue crosses in Fig. 2. Unfortunately, the linearization includes an eigenvalue of 1, which corresponds to the shift invariance in the phase angles and is characteristic for all AC power systems. In the xy coordinates chosen, this angle shift invariance manifests as rotations of the phasors in the xy plane. To remove this angle shift invariance from the identification, the swing bus angle is selected as a reference, and all the phase angles in the training data are preprocessed as differences to the reference angle. As a result, the DMDc problem satisfies condition 1 in Definition 1.

B. Model Order Selection

From our test, the model order cannot be selected by finding a gap in the distribution of the singular values of the data matrix $\boldsymbol{\Omega}$. However, from the uniqueness discussion when the order is much higher than the underlying system there will be additional eigenvalues of 1 from $\hat{\mathbf{A}}$. In this example, we choose the model order to be 18 where the identified eigenvalue is shown in Fig. 2. Another case where the model order is much higher than the underlying system is shown in Fig. 3, where we see that additional incorrect modes are present in the second model.

C. Eigenvalue and Eigenvector Verifications

To compare DMDc eigenvalues and eigenvectors to those of the true system, the DAE converted into a discrete-time linear system at the first of the two load conditions in the training data. For the selected model order of 18, the eigenvalues of DAE linearization and those identified by DMDc are compared in Fig. 2.

Furthermore, the corresponding elements of the eigenvectors associated with the eigenvalues 1 to 5 are compared between DAE linearization and DMDc using Modal Assurance Criterion (MAC) [15] as shown in Fig. 4. Two vectors are more similar when their MAC is closer to 1. The diagonal elements in Fig. 4 are the highest confirming that modes 1 to 4 are correctly identified through DMDc. Since the fifth eigenvalue is not identified by DMDc, the eigenvectors of DMDc that are associated with eigenvalues #3 and #4 have a slightly higher MAC with eigenvector #5 of DAE linearization. In Fig. 5, the eigenvectors of DAE and DMDc associated with eigenvalue 1 are plotted.

D. Time-Domain Predictions

Figures 6 and 7 show the predictions of voltages at bus 1 under small and larger load change conditions. For larger load changes, the frequency contents of the transient response is farther from the local transient response learned by DMDc.

To evaluate the capability of the DMDc model to predict transient dynamics, 169 test cases are used to compare the

979-8-3503-1360-4/24/$31.00 ©2024 IEEE

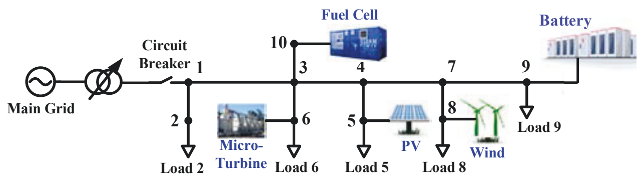

Fig. 1. A typical microgrid test system.

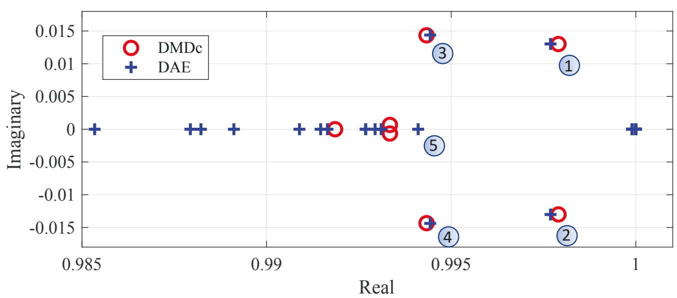

Fig. 2. Eigenvalue comparison for truncation order 18

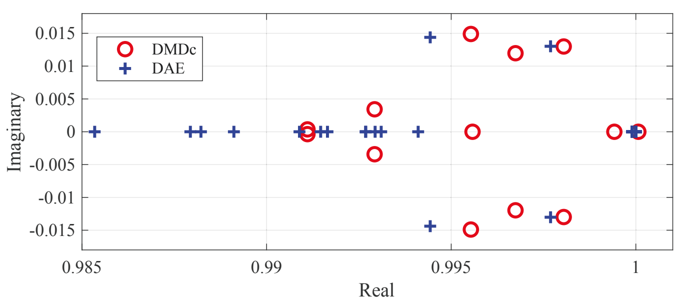

Fig. 3. Eigenvalue comparison for truncation order 35

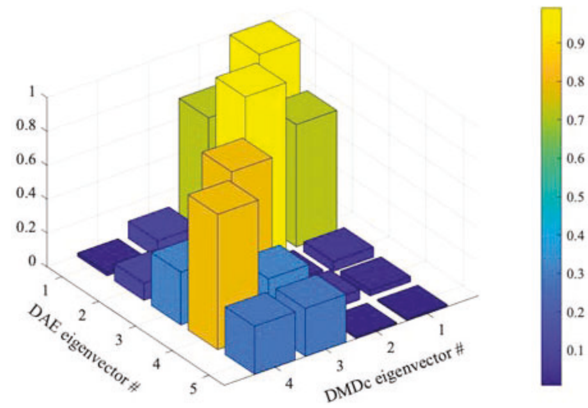

Fig. 4. Modal assurance criterion between eigenvectors corresponding to eigenvalues #1 to #5 in Fig. 2

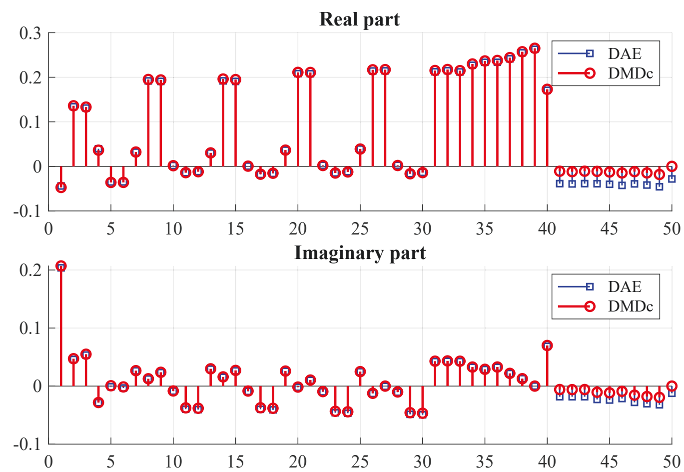

Fig. 5. DMDc eigenvector corresponding to eigenvalue 1 in Fig. 2 compared to DAE linearization

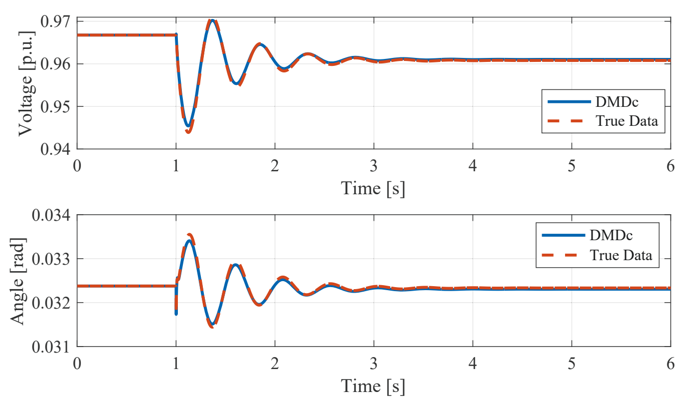

Fig. 6. Voltage prediction after Load 5 changes by -40% and Load 6 changes by 60%

DMDc predictions and the simulated trajectories. Starting from the nominal condition, Load 5 and Load 6 are stepped to between -100% and 140% of the respective nominal loads with an interval of 20%. In Fig. 8, the contour log of squared errors for all 169 cases in the same prediction period of ten seconds are plotted. The nominal equilibrium point is marked by cross and the training data comprise of load changes marked by the two arrows. The locally linearized dynamics of the microgrid is correctly captured in the local region of 20% load changes compared to the nominal condition, while the nonlinear dynamics becomes steadily different from the DMDc model when much larger load changes are introduced.

IV. Conclusions

A data-driven modeling approach for microgrids under disturbances is developed based on DMDc. Conditions on the training data and the underlying model is discussed to ensure the uniqueness of the solution, and the testing results on a microgrid test system shows the ability of the method to recover linear modes during microgrid transients due to load changes. A future direction is to develop successive DMDc models at different nominal conditions with applications for data-driven model-predictive control.

V. Acknowledgment

This work is supported by National Science Foundation under the award DMS-2229435.

979-8-3503-1360-4/24/$31.00 ©2024 IEEE

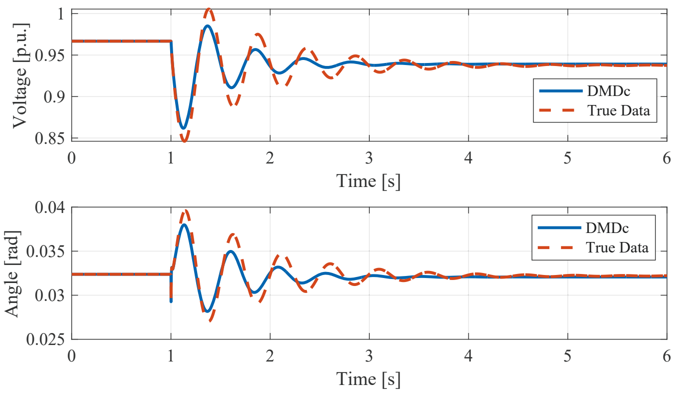

Fig. 7. Voltage prediction after Load 5 changes by 80% and Load 6 change by 100%

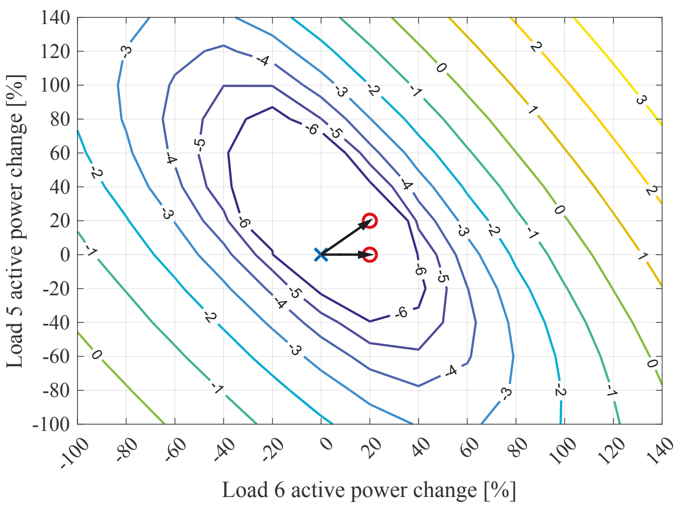

Fig. 8. Log of squared errors for prediction of load changes from the nominal condition

VI. Appendix

A. DAE Linearization

Consider a DAE system consisting of differential equations $\dot{\mathbf{x}} = \mathbf{f}(\mathbf{x}, \mathbf{y}, \mathbf{u})$ and constraint $\mathbf{0} = \mathbf{g}(\mathbf{x}, \mathbf{y}, \mathbf{u})$ with state variables $\mathbf{x}$, algebraic variables $\mathbf{y}$, and input $\mathbf{u}$. The linearized system at an equilibrium point $(\bar{\mathbf{x}}, \bar{\mathbf{y}})$ can be formulated as

$$\begin{bmatrix} \Delta\dot{\mathbf{x}} \\ \Delta\dot{\mathbf{y}} \end{bmatrix} = \begin{bmatrix} \mathbf{A}_c - \mathbf{B}_c \mathbf{D}^{-1}{}_c \mathbf{C}_c & \mathbf{0} \\ -\mathbf{D}^{-1}{}_c \mathbf{C}_c \mathbf{A}_c & -\mathbf{D}^{-1}{}_c \mathbf{C}_c \mathbf{B}_c \end{bmatrix} \begin{bmatrix} \Delta\mathbf{x} \\ \Delta\mathbf{y} \end{bmatrix} \quad (12)$$

where $\mathbf{A}_c$, $\mathbf{B}_c$, $\mathbf{C}_c$, $\mathbf{D}_c$ are the partial derivatives of $\mathbf{f}$ and $\mathbf{g}$ with respect to $\mathbf{x}$ and $\mathbf{y}$, which are functions of $\mathbf{u}$. From (12), assume that $(\bar{\mathbf{x}}, \bar{\mathbf{y}})$ changes linearly with $\mathbf{u}$, and $\mathbf{A}_c$ to $\mathbf{D}_c$ stay constant. One can get the form (1).

B. Proof Sketch of Theorem 1

First we define the $(p+1) \times s$ Vandermonde matrices $\mathbf{\Lambda}_p$ as

$$\mathbf{\Lambda}_p = \begin{bmatrix} 1 & 1 & \dots & 1 \\ \lambda_1 & \lambda_2 & \dots & \lambda_s \\ \vdots & \vdots & \vdots & \vdots \\ \lambda_1^p & \lambda_2^p & \dots & \lambda_s^p \end{bmatrix}, \quad (13)$$

and the $n \times s$ eigenvector matrix $\mathbf{V} = [\mathbf{v}_1 \dots \mathbf{v}_s]$. From Definition 1, we may write the matrix of state snapshots as

$$\mathbf{X} - \begin{bmatrix} \mathbf{c}_1 & \cdots & \mathbf{c}_h \end{bmatrix} \begin{bmatrix} \mathbf{1}_{m_1}^\mathsf{T} & & \\ & \ddots & \\ & & \mathbf{1}_{m_h}^\mathsf{T} \end{bmatrix} = \mathbf{V} \begin{bmatrix} \mathbf{M}_1 & \cdots & \mathbf{M}_h \end{bmatrix} \begin{bmatrix} \mathbf{\Lambda}_{m_1}^\mathsf{T} & & \\ & \ddots & \\ & & \mathbf{\Lambda}_{m_h}^\mathsf{T} \end{bmatrix} \quad (14)$$

where $\mathbf{M}_i$ are diagonal matrices such that $\mathbf{x}_{m_i'} - \mathbf{c}_i = \mathbf{V}\mathbf{M}_i \mathbf{1}_s$, $i = 1, \dots, h$. Then using Theorem 4.7 in [12] on each m_i columns having constant input on each side of the equation, we have that $\mathbf{c}_i$'s are unique and so are the r distinct nonzero eigenvalues λ_k and their corresponding eigenvectors are unique up to scaling.

References

[1] Y. Li, P. Zhang, and M. Yue, "Networked microgrid stability through distributed formal analysis," *Applied energy*, vol. 228, pp. 279–288, 2018.

[2] A. A. Ademola-Idowu, *Frequency Stability in Low-Inertia Power Systems*. University of Washington, 2020.

[3] M. R. Overlin, C. Smith, and J. L. Kirtley, "A hybrid algorithm for parameter estimation (hape) for dynamic constant power loads," *IEEE Transactions on Industrial Electronics*, 2020.

[4] P. N. Papadopoulos, T. A. Papadopoulos, P. Crolla, A. J. Roscoe, G. K. Papagiannis, and G. M. Burt, "Black-box dynamic equivalent model for microgrids using measurement data," *IET Generation, Transmission & Distribution*, vol. 8, no. 5, pp. 851–861, 2014.

[5] B. Zaker, G. B. Gharehpetian, and M. Karrari, "A novel measurement-based dynamic equivalent model of grid-connected microgrids," *IEEE Transactions on Industrial Informatics*, vol. 15, no. 4, pp. 2032–2043, 2018.

[6] A. Firdaus and S. Mishra, "Empirical mode decomposition based identification of low frequency modes in inverter based microgrid," in *2018 IEEE Industry Applications Society Annual Meeting (IAS)*. IEEE, 2018, pp. 1–6.

[7] N. Zhou, J. W. Pierre, and J. F. Hauer, "Initial results in power system identification from injected probing signals using a subspace method," *IEEE Transactions on power systems*, vol. 21, no. 3, pp. 1296–1302, 2006.

[8] P. J. Schmid, "Dynamic mode decomposition of numerical and experimental data," *Journal of fluid mechanics*, vol. 656, pp. 5–28, 2010.

[9] J. L. Proctor, S. L. Brunton, and J. N. Kutz, "Dynamic mode decomposition with control," *SIAM Journal on Applied Dynamical Systems*, vol. 15, no. 1, pp. 142–161, 2016.

[10] D. Goswami and D. A. Paley, "Bilinearization, reachability, and optimal control of control-affine nonlinear systems: A koopman spectral approach," *IEEE Transactions on Automatic Control*, 2021.

[11] C. L. Lawson and R. J. Hanson, *Solving least squares problems*. SIAM, 1995.

[12] S. M. Hirsh, K. D. Harris, J. N. Kutz, and B. W. Brunton, "Centering data improves the dynamic mode decomposition," *SIAM Journal on Applied Dynamical Systems*, vol. 19, no. 3, pp. 1920–1955, 2020.

[13] S. Chakrabarti, "Notes on power system voltage stability," *Dept. of EE, IIT, Kanpur http://home. iitk. ac. in/~ saikatc/EE632_files/VS_SC. pdf (assessed on 1st Nov 2011)*, 2011.

[14] Y. Li, *Cyber-Physical Microgrids*. Springer Nature, 2021.

[15] R. J. Allemang, "The modal assurance criterion–twenty years of use and abuse," *Sound and vibration*, vol. 37, no. 8, pp. 14–23, 2003.

979-8-3503-1360-4/24/$31.00 ©2024 IEEE